Molecular Neurobiology
https://doi.org/10.1007/s12035-018-1004-1

α_{2A}- and α_{2C}-Adrenoceptors as Potential Targets for Dopamine and Dopamine Receptor Ligands

Marta Sánchez-Soto[1,2,3] · Verònica Casadó-Anguera[2,3] · Hideaki Yano[1] · Brian Joseph Bender[4,5] · Ning-Sheng Cai[1] · Estefanía Moreno[2,3] · Enric I. Canela[2,3] · Antoni Cortés[2,3] · Jens Meiler[4,5] · Vicent Casadó[2,3] · Sergi Ferré[1]

Received: 14 December 2017 / Accepted: 7 March 2018
© This is a U.S. Government work and not under copyright protection in the US; foreign copyright protection may apply 2018

Abstract

The poor norepinephrine innervation and high density of Gi/o-coupled α_{2A}- and α_{2C}-adrenoceptors in the striatum and the dense striatal dopamine innervation have prompted the possibility that dopamine could be an effective adrenoceptor ligand. Nevertheless, the reported adrenoceptor agonistic properties of dopamine are still inconclusive. In this study, we analyzed the binding of norepinephrine, dopamine, and several compounds reported as selective dopamine D_2-like receptor ligands, such as the D_3 receptor agonist 7-OH-PIPAT and the D_4 receptor agonist RO-105824, to α_2-adrenoceptors in cortical and striatal tissue, which express α_{2A}-adrenoceptors and both α_{2A}- and α_{2C}-adrenoceptors, respectively. The affinity of dopamine for α_2-adrenoceptors was found to be similar to that for D_1-like and D_2-like receptors. Moreover, the exogenous dopamine receptor ligands also showed high affinity for α_{2A}- and α_{2C}-adrenoceptors. Their ability to activate Gi/o proteins through α_{2A}- and α_{2C}-adrenoceptors was also analyzed in transfected cells with bioluminescent resonance energy transfer techniques. The relative ligand potencies and efficacies were dependent on the Gi/o protein subtype. Furthermore, dopamine binding to α_2-adrenoceptors was functional, inducing changes in dynamic mass redistribution, adenylyl cyclase activity, and ERK1/2 phosphorylation. Binding events were further studied with computer modeling of ligand docking. Docking of dopamine at α_{2A}- and α_{2C}-adrenoceptors was nearly identical to its binding to the crystallized D_3 receptor. Therefore, we provide conclusive evidence that α_{2A}- and α_{2C}-adrenoceptors are functional receptors for norepinephrine, dopamine, and other previously assumed selective D_2-like receptor ligands, which calls for revisiting previous studies with those ligands.

Keywords α_2-Adrenoceptors · BRET · DMR · Adenylyl cyclase · ERK1/2 phosphorylation · Docking

Marta Sánchez-Soto and Verònica Casadó-Anguera contributed equally to this work.

✉ Vicent Casadó
vcasado@ub.edu

✉ Sergi Ferré
sferre@Intra.nida.nih.gov

[1] Integrative Neurobiology Section, National Institute on Drug Abuse, Intramural Research Program, National Institutes of Health, Triad Technology Building, 333 Cassell Drive, Baltimore, MD 21224, USA

[2] Department of Biochemistry and Molecular Biomedicine, Faculty of Biology, University of Barcelona, Diagonal 643, 08028 Barcelona, Spain

[3] Centro de Investigación Biomédica en Red sobre Enfermedades Neurodegenerativas (CIBERNED), Institute of Biomedicine, University of Barcelona, Barcelona, Spain

[4] Department of Pharmacology, Vanderbilt University, Nashville, TN 37232, USA

[5] Center for Structural Biology, Vanderbilt University, Nashville, TN 37232, USA

Introduction

The neurotransmitter norepinephrine (NE) binds and activates three subfamilies of adrenoceptors: α_1-adrenoceptors, subdivided into α_{1A}, α_{1B}, and α_{1D}; α_2-adrenoceptors, subdivided into α_{2A}, α_{2B}, and α_{2C}; and β-adrenoceptors, subdivided into β_1, β_2, and β_3 [1]. Classically, α_1-, α_2- and β-adrenoceptors couple to Gq/11, Gi/o, and Gs, respectively [1, 2]. In mammalian species, α_{2A} is the main subtype in most brain regions whereas α_{2B} subtype has a limited distribution and is mostly expressed in the thalamus [3, 4]. The α_{2C} subtype is found with particularly high density in the striatum [5, 6] with a moderately lower density than α_{2A} [7, 8]. The high density of dorsal striatal α_{2A}- and α_{2C}-adrenoceptors prompted a fundamental question in view of the well-known paucity of striatal noradrenergic terminals [9–11] and the concomitant low extracellular levels of striatal NE [12]. Yet, a series of studies indicate that both types of receptors are fully

functional in the striatum, where they seem to be localized mostly postsynaptically, preferentially in GABAergic striatal efferent neurons [13, 14]. There is also evidence for α_{2A}-adrenoceptors playing a role as autoreceptors localized in the sparse striatal noradrenergic terminals [15]. It was postulated by Zhang et al. [16] that dopamine (DA) could provide the endogenous neurotransmitter for striatal α_2-adrenoceptors. In transfected mammalian cells, using radioligand binding experiments, they found only a small preferential affinity of NE versus DA at both α_{2A}- and α_{2C}-adrenoceptors. Similar results were more recently obtained from radioligand binding studies using transfected mammalian and insect cell lines [17] and with radioligand binding and autoradiographic experiments in the bird and rat brain with a non-selective α_2-adrenoceptor ligand [18]. However, Zhang et al. [16] reported a much lower potency of DA (in the micromolar range) than NE (in the nanomolar range) at the level of α_{2C}-adrenoceptor-mediated signaling (modulation of forskolin-induced adenylyl cyclase activation).

Due to the mismatch between dopaminergic and noradrenergic innervation and the density of their receptors in several brain areas, the controversy about the differential binding affinity of DA versus NE on adrenoceptors, and the potential functional efficacy of this binding, we wanted to study in detail the ability of DA and several synthetic DA receptor ligands to bind to the orthosteric site of α_2-adrenoceptors in transfected cells and in the sheep brain. Moreover, we further analyzed the ability of these ligands to generate functional responses: activation of G proteins, inhibition of cAMP accumulation, and ERK1/2 phosphorylation. In the present study, we first analyzed the ability of DA and several DA receptor ligands to bind to α_2-adrenoceptors in cortical tissue, which predominantly expresses α_{2A}-adrenoceptors, and in striatal tissue, which expresses both α_{2A}- and α_{2C}-adrenoceptors. We also studied the potential dopaminergic function of α_{2A}- and α_{2C}-adrenoceptors using the same methodology that recently allowed us to demonstrate the potent activation of all Gi/o-coupled DA D_2-like receptors by NE [19]. This methodology consists on sensitive bioluminescence resonance energy transfer (BRET)-based techniques that allow detection of ligand-dependent interactions between specific receptors and specific G proteins (G protein activation) or receptor-induced activation of effectors (adenylyl cyclase activity) in living cells [19]. Moreover, we compared the ability of NE, DA, and DA receptor ligands to modulate dynamic mass redistribution (DMR) and to activate MAPK signaling. Lastly, we modeled the binding of DA at α_{2A}- and α_{2C}-adrenoceptors, as compared to its binding to the crystallized D_3 receptor. Our results provide conclusive evidence for α_{2A}- and α_{2C}-adrenoceptors being not only NE but also DA receptors and common targets for other D_2-like receptor ligands.

Materials and Methods

DNA Constructs and Transfection

For BRET experiments, human receptor constructs were used for α_{2A}- and α_{2C}-adrenoceptors (cDNA Resource Center). The following human G protein constructs were used: Gαi1-, Gαi2-, Gαi3-, Gαo1-, or Gαo2-Renilla luciferase 8 (RLuc8) with RLuc8 inserted at position 91, untagged Gβ1, and Gγ2 fused to full-length mVenus at its N terminus. The Gα-RLuc8 constructs were kindly provided by Céline Galés (INSERM, Toulouse, France). The cAMP sensor using YFP-Epac-Rluc (CAMYEL) biosensor was obtained from the American Type Culture Collection (no. MBA-277; ATCC, Manassas, VA, USA) [20]. All the constructs were confirmed by sequencing analysis. A constant amount of plasmid cDNA (0.5 μg Gα-RLuc8, 4.5 μg Gβ1, 5 μg Gγ2-mVenus, and 5 μg receptor) was transfected into HEK-293T cells using polyethylenimine (Sigma-Aldrich) in a 1:2 ratio in 10-cm dishes. Cells were maintained in culture with Dulbecco's modified Eagle's medium supplemented with 10% fetal bovine serum and kept in an incubator at 37 °C and 5% CO_2. The transfected amount and ratio among the receptor and heterotrimeric G proteins were tested for optimized dynamic range in drug-induced BRET. HEK-293T cells were also used in BRET experiments for determination of adenylyl cyclase inhibition (see below). For DMR and ERK1/2 phosphorylation assays, Chinese hamster ovary (CHO) cells were grown in minimum essential medium (MEMα; Gibco) supplemented with 2 mM L-glutamine, 100 μg/ml sodium pyruvate, MEM non-essential amino acid solution (1:100), 100 U/ml penicillin/streptomycin, and 5% (*v*/*v*) of heat-inactivated fetal bovine serum. These cells were transfected with human α_{2A}-RLuc8 receptor using polyethylenimine in a 1:2 ratio in 25-cm^2 cell culture flasks. All experiments were performed approximately 48 h after transfection.

BRET

BRET assays were performed to detect receptor ligand-induced events for Gi/o protein activation. Gi/o protein activation assay used RLuc-fused Gαi/o protein subunit and mVenus-fused Gγ2 protein for BRET pair. Receptor and untagged Gβ1 constructs were co-transfected. As reported previously [19, 20], cells were harvested, washed, and resuspended in phosphate-buffered saline. Approximately 200,000 cells/well were distributed in 96-well plates, and 5 μM coelenterazine H (substrate for luciferase) was added to each well. One minute after the addition of coelenterazine H, ligands (DA, NE, clonidine, quinpirole, 7-OH-PIPAT, and RO-105824) were added to each well. Antagonists were added 10 min before coelenterazine. The fluorescence of the acceptor was quantified (excitation at 500 nm and emission at

540 nm for 1-s recordings) in Mithras LB940 (Berthold Technologies, Bad Wildbad, Germany) to confirm the constant expression levels across experiments. In parallel, the BRET signal from the same batch of cells was determined as the ratio of the light emitted by mVenus (510–540 nm) over that emitted by RLuc (485 nm). G protein activation was calculated as the BRET change (BRET ratio for the corresponding drug minus the BRET ratio in the absence of the drug) observed 10 min after the addition of the ligands. E_{max} values were expressed as the percentage of the effect of each ligand over the effect of NE. BRET curves were analyzed by nonlinear regression using the commercial Prism 4 (GraphPad Software).

DMR

A global cell signaling profile or DMR was measured using an EnSpire Multimode Plate Reader (PerkinElmer, Waltham, MA, USA). This label-free approach uses refractive waveguide grating optical biosensors, integrated into 384-well microplates. Changes in local optical density are measured in a detection zone up to 150 nm above the surface of the sensor. Cellular mass movements induced upon receptor activation are detected by illuminating the underside of the biosensor with polychromatic light and measured as changes in the wavelength of the reflected monochromatic light. These changes are a function of the refraction index. The magnitude of this wavelength shift (in picometers) is directly proportional to the amount of DMR. Briefly, after 24 h of CHO cell transfection with α_{2A}-RLuc8 receptor, cells were resuspended and seeded at a density of 7000 cells per well in 384-well sensor microplates in 30 μl growing media and cultured for 24 h at 37 °C and 5% CO_2, to obtain monolayers at 70–80% confluency. Before starting the assay, cells were washed twice with assay buffer (MEMα supplemented with 20 mM HEPES, pH 7.15, 0.1% DMSO, and 0.1% BSA) and incubated 2 h in 40 μl per well in the reader at 24 °C. Hereafter, the sensor plate was scanned, and a baseline optical signature was recorded for 10 min before adding 10 μl of the agonist dissolved in assay buffer and recorded for 90 min. Kinetic results were analyzed using EnSpire Workstation Software v 4.10.

Adenylyl Cyclase Activity

BRET assays were performed to detect receptor ligand-induced adenylyl cyclase activity. This assay used the CAMYEL biosensor construct which contains RLuc and YFP. The biosensor detects the conformational changes in Epac that are induced upon its binding to cAMP. The conformational change triggered by an increase in cAMP induced by forskolin results in a decrease in BRET due to the relative orientation change between donor and acceptor. A decrease in forskolin-induced cAMP levels is therefore observed as an increase in BRET [21]. To study Gαi-dependent inhibition activity, cells were treated as described above but pre-stimulated for 10 min with 1 μM forskolin (Sigma-Aldrich), in the presence of 10 μM propranolol 10 min before sample reading to control for activation of endogenous β-adrenergic receptors (see "Results").

ERK1/2 Phosphorylation

CHO cells were transfected with α_{2A}-RLuc8 receptor, obtaining a transfection of about 0.3 pmol/mg protein. The day of the experiment, cells were starved by treating them with serum-free media for 4 h at 37 °C. After that, cells were incubated with the indicated agonist for 5 min at 37 °C. Then, cells were rinsed with ice-cold phosphate-buffered saline and lysed by adding 200 ml ice-cold lysis buffer (50 mM Tris-HCl (pH 7.4), 50 mM NaF, 150 mM NaCl, 45 mM β-glycerophosphate, 1% Triton X-100, 20 mM phenylarsine oxide, 0.4 mM $NaVO_4$, and protease inhibitor cocktail). The cellular debris was removed by centrifugation at 13,000*g* for 5 min at 4 °C, and the protein was quantified. To determine the level of ERK1/2 phosphorylation, equivalent amounts of protein were separated by electrophoresis on a denaturing 10% SDS polyacrylamide gel and transferred onto polyvinylidene fluoride membranes. Odyssey blocking buffer (LI-COR Biosciences, Lincoln, NE, USA) was then added, and the membrane was rocked for 90 min. The membranes were then probed with a mixture of a mouse anti-phospho-ERK1/2 antibody (1:2500; Sigma-Aldrich) and rabbit anti-ERK1/2 antibody that recognizes both phosphorylated and non-phosphorylated ERK1/2 (1:40,000; Sigma-Aldrich) overnight at 4 °C. The 42- and 44-kDa bands corresponding to ERK1 and ERK2 were visualized by the addition of a mixture of IRDye 800 (anti-mouse) antibody (1:10,000; Sigma-Aldrich) and IRDye 680 (anti-rabbit) antibody (1:10,000; Sigma-Aldrich) for 2 h and scanned by the Odyssey infrared scanner (LICOR Biosciences). Band densities were quantified using the scanner software and exported to Excel (Microsoft, Redmond, WA, USA). The level of phosphorylated ERK1/2 isoforms was normalized for differences in loading using the total ERK1/2 protein band intensities.

Radioligand Binding

Brains of male and female sheep of 4–6 months old were freshly obtained from the local slaughterhouse. Brain tissues (cortex and dorsal striatum) and HEK-293T cell suspensions were disrupted with a Polytron homogenizer (PTA 20 TS rotor, setting 3; Kinematica, Basel, Switzerland) for two 5-s periods in 10 volumes of 50 mM Tris-HCl buffer, pH 7.4, containing a proteinase

inhibitor cocktail (Sigma, St. Louis, MO, USA). Membranes were obtained by centrifugation twice at 105,000*g* for 45 min at 4 °C. The pellet was stored at − 80 °C, washed once more as described above, and resuspended in 50 mM Tris-HCl buffer for immediate use. Membrane protein was quantified by the bicinchoninic acid method (Pierce Chemical Co., Rockford, IL, USA) using bovine serum albumin dilutions as standard. Binding experiments were performed with membrane suspensions at room temperature in 50 mM Tris-HCl buffer, pH 7.4, containing 10 mM $MgCl_2$. For competition-binding assays, membrane suspensions (0.2 mg of protein/ml) were incubated for 2 h with a constant-free concentration of 0.9 nM of the α_2R-antagonist [^{3}H]RX821002 or 1.3 nM of the D_1-like receptor antagonist [^{3}H]SCH 23390 or 0.8 nM of the D_2-like receptor antagonist [^{3}H]YM-09151-2 and increasing concentrations of each tested ligand: NE, DA, clonidine, 7-OH-PIPAT, quinpirole, and RO-105824. For α_2R saturation-binding assays, membrane suspensions (0.2 mg of protein/ml) were incubated for 3 h at room temperature in 50 mM Tris-HCl buffer, pH 7.4, containing 10 mM $MgCl_2$ with increasing concentrations of the α_2R-antagonist [^{3}H]RX821002. Non-specific binding was determined in the presence of 10 μM of the non-radiolabeled antagonist RX821002 (for α_2R) or 30 μM of DA (for D_1R and D_2R). In all cases, free and membrane-bound ligands were separated by rapid filtration of 500-μl aliquots in a cell harvester (Brandel, Gaithersburg, MD, USA) through Whatman GF/C filters embedded in 0.3% polyethylenimine that were subsequently washed for 5 s with 5 ml of ice-cold 50 mM Tris-HCl buffer. The filters were incubated with 10 ml of Ecoscint H scintillation cocktail (National Diagnostics, Atlanta, GA, USA) overnight at room temperature, and radioactivity counts were determined using a Tri-Carb 2800 TR scintillation counter (PerkinElmer) with an efficiency of 62%.

Binding Data Analysis

Data were analyzed according to the "two-state dimer model" of Casadó et al. [22]. The model assumes GPCR dimers as a main functional unit and provides a more robust analysis of parameters obtained from saturation and competition experiments with orthosteric ligands, as compared with the commonly used "two-independent site model" [22, 23]. In saturation experiments with the radioligand, the model analyzes the total number of radioligand binding sites (B_{max}; more specifically, it calculates R_T, the total number of dimers, where $B_{max} = 2R_T$), the affinity of the radioligand for the first protomer in the unoccupied dimer (K_{DA1}), the affinity of the radioligand for the second protomer when the first protomer is already occupied by the radioligand (K_{DA2}), and an index of cooperativity of the radioligand (D_{CA}). A positive or negative value of D_{CA} implies either an increase or a decrease in affinity of K_{DA2} versus K_{DA1}, and its absolute value provides a measure of the degree of increase or decrease in affinity. In competition experiments, the model analyzes the interactions of the radioligand with a competing ligand and it provides the affinity of the competing ligand for the first protomer in the unoccupied dimer (K_{DB1}), the affinity of the competing ligand for the second protomer when the first protomer is already occupied by the competing ligand (K_{DB2}) or the radioligand (K_{DAB}), and an index of cooperativity of the competing ligand (D_{CB}). A positive or negative value of D_{CB} implies either an increase or a decrease in affinity of K_{DB2} versus K_{DB1}, and its absolute value provides a measure of the degree of increase or decrease in affinity.

Radioligand competition and saturation curves were analyzed by non-linear regression using the commercial GraFit curve-fitting software (Erithacus Software, Surrey, UK), by fitting the binding data to the mechanistic two-state dimer receptor model, as described in detail elsewhere [24]. The equation describing the saturation experiment with the radioligand A in non-cooperative conditions ($K_{DA2} / K_{DA1} = 4$) is as follows: $A_{bound} = 2AR_T / (2K_{DA1} + A)$, where A represents the radioligand concentration. To calculate the macroscopic equilibrium dissociation constants from competition experiments, the following general equation must be applied: $A_{bound} = (K_{DA2}A + 2A^2 + K_{DA2}AB / K_{DAB})R_T / (K_{DA1}K_{DA2} + K_{DA2}A + A^2 + K_{DA2}AB / K_{DAB} + K_{DA1}K_{DA2}B / K_{DB1} + K_{DA1}K_{DA2}B^2 / (K_{DB1}K_{DB2}))$, where B represents the assayed competing compound concentration (F). For A, the non-cooperative and non-allosteric modulation between A and B, the equation is simplified due to the fact that $K_{DA2} = 4K_{DA1}$ and $K_{DAB} = 2K_{DB1}$; $A_{bound} = (4K_{DA1}A + 2A^2 + 2K_{DA1}AB / K_{DB1})R_T / (4K_{DA1}^2 + 4K_{DA1}A + A^2 + 2K_{DA1}AB / K_{DB1} + 4K_{DA1}^2B / K_{DB1} + 4K_{DA1}^2B^2 / (K_{DB1}K_{DB2}))$. For A and B, the non-cooperative and non-allosteric modulation between A and B, the equation can be simplified due to the fact that $K_{DA2} = 4K_{DA1}$, $K_{DB2} = 4K_{DB1}$, and $K_{DAB} = 2K_{DB1}$; $A_{bound} = (4K_{DA1}A + 2A^2 + 2K_{DA1}AB / K_{DB1})R_T / (4K_{DA1}^2 + 4K_{DA1}A + A^2 + 2K_{DA1}AB / K_{DB1} + 4K_{DA1}^2B / K_{DB1} + K_{DA1}^2B^2 / K_{DB1}^2)$.

Statistical Analysis

In binding assays, goodness of fit was tested according to reduced chi-square value given by the regression program. The test of significance for two different model population variances was based upon the F-distribution. Using this F-test, a probability greater than 95% ($p < 0.05$) was considered to be the criterion to select a more complex model (cooperativity) over the simplest one (non-cooperativity). In all cases, a probability of less than 70% ($p > 0.30$) resulted when one model was not significantly better than the other. In all cases, results

are given as parameter values ± SEM and statistical differences were analyzed with Prism 4.

Drugs

Dopamine hydrochloride and L-(−)-norepinephrine (+)-bitartrate salt monohydrate were purchased from Sigma. (−)-Quinpirole hydrochloride, clonidine hydrochloride, 7-OH-PIPAT maleate, RO-105824 dihydrochloride, RX821002, and yohimbine hydrochloride were purchased from Tocris. $[^3H]$RX821002 (63.9 Ci/mmol), $[^3H]$SCH 23390 (81.9 Ci/mmol), and $[^3H]$YM-09151-2 (84.4 Ci/mmol) were from PerkinElmer. Pertussis toxin was purchased from Sigma.

Homology Modeling of α_{2A}- and α_{2C}-Adrenoceptors

Homology models of α_{2A}- and α_{2C}-adrenoceptors were constructed from multiple templates using RosettaCM [25] with a protocol previously described [26]. Sequences of each adrenoceptor were aligned with sequences of the following receptors: D_3 (PDB ID: 3PBL [27]), β_1 (PDB ID: 4BVN [28]), β_2 (PDB ID: 2RH1 [29]), $5HT_{1B}$ (PDB ID: 4IAR [30]), and $5HT_{2B}$ (PDB ID: 4IB4 [31]) using BLAST and were modified to ensure alignment of secondary structure elements and conserved residues. The N-terminus was truncated through residues 28 and 46 and the C-terminus was deleted after residues 442 and 456, respectively. Additionally, the long intracellular loop 3 was deleted at residues 229–372 in α_{2A} and 243–381 in α_{2C} and replaced with an eight-residue poly-Gly linker. These sequences were threaded onto each template and hybridized to generate full-length, energy-minimized structures. Models were clustered using automatic radius detection in Rosetta, and the low-energy cluster centers from the top five clusters were selected for additional modeling.

Protein-Ligand Docking

The tridimensional structure of DA was obtained from PubChem (ID 3713609). Conformers of DA were generated using the BCL [32]. To identify the initial starting coordinates for ligand docking, homology models were aligned with the crystal structure of β_2-adrenoceptor (PDB ID: 4LDO (33)) and DA was aligned with the crystallized ligand. Ligand docking was performed in RosettaLigand using the small perturbation of ligand position protocol and swapping of ligand conformers [33, 34]. One thousand models for each protein-ligand complex were generated. Models were sorted initially by total energy and then culled to the top 5% of models by interface energies for analysis. Per-residue ΔΔG analysis was performed to identify residues involved in ligand binding.

Results

Binding of DA and DA Receptor Ligands to α_2-Adrenoceptors in Cortical and Striatal Tissue

First, we analyzed the ability of NE, DA, the non-selective α-adrenoceptor agonist clonidine, the non-selective D_2-D_3-D_4 receptor agonist quinpirole, the selective D_3 receptor agonist 7-OH-PIPAT, and the selective D_4 receptor agonist RO-105824 to displace the binding of the non-selective α_2-adrenoceptor antagonist radioligand $[^3H]$RX821002 in membrane preparations from the sheep cortex and striatum with competitive inhibition experiments. See "Materials and Methods" and refs. [22–24] for description of the variables. Saturation experiments with $[^3H]$RX821002 for cortical and striatal tissue provided B_{max} values for α_2-adrenoceptors of 0.33 ± 0.02 and 0.13 ± 0.02 pmol/mg protein and affinity values (K_{DA1}) of 0.06 ± 0.01 and 0.07 ± 0.01 nM ($n = 4$–8), respectively. This implies that the density of α_2-adrenoceptors in the cortex, which is mostly represented by α_{2A}-adrenoceptors [3, 4], is three times higher than that in the striatum, which expresses similar densities for both α_{2A}- and α_{2C}-adrenoceptors [8]. To test the binding selectivity of $[^3H]$RX821002 for α_2-adrenoceptors and not for D_2-like receptors, we developed competition experiments of the D_2-like receptor antagonist $[^3H]$YM-09151-2 with increasing concentrations of unlabeled RX821002 in sheep striatal membranes. RX821002 did not displace the radioligand binding at any concentration up to 10 μM (Fig. 1a). The same experiments were also performed in membranes from HEK-293T cells stably transfected with human D_2, D_3, or D_4 receptors, with identical results (data not shown). These results demonstrate that the radioligand $[^3H]$RX821002 does not bind to D_2-like receptors.

Competition experiments of $[^3H]$RX821002 with NE, DA, clonidine, and the D_2-like receptor ligands in cortical and striatal sheep membranes are shown in Fig. 2a, b, respectively, and the K_{DB1}, K_{DB2}, and D_{CB} values obtained are presented in Table 1. In both tissues, NE, DA, and clonidine showed high affinity for $[^3H]$RX821002 binding sites with an order of potency of clonidine > NE > DA (Fig. 2). The three ligands showed negative cooperativity (negative D_{CB} values). The affinity of NE was higher in the cortex than in the striatum, with higher striatal K_{DB1}, K_{DB2}, and D_{CB} values (stronger negative cooperativity) (Table 1). The affinity of DA was very similar in both tissues, with similar K_{DB1} values and a moderately but significantly higher K_{DB2} value in the striatum, resulting in similar D_{CB} values (Table 1). The affinity of clonidine was also higher in the cortex, with a significantly higher striatal K_{DB1} value and similar D_{CB} values (Table 1). 7-OH-PIPAT and quinpirole also displaced $[^3H]$RX821002 binding with nanomolar and submicromolar affinities, respectively (Table 1, Fig. 2). Interestingly, 7-OH-PIPAT showed negative cooperativity in the cortex, but not in the striatum. The only measurable affinity parameter of 7-OH-PIPAT in the striatum, K_{DB1}, was significantly higher than that in the

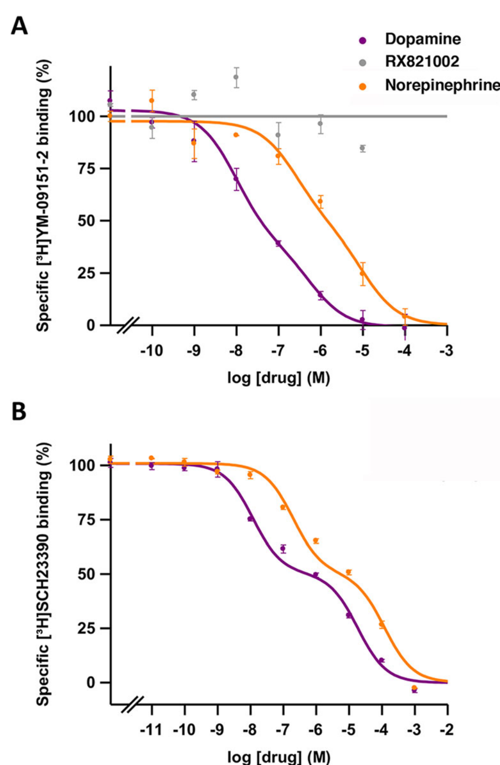

Fig. 1 Radioligand binding to D_2-like and D_1-like receptors in the brain striatum. Representative competition curves of D_2-like receptor antagonist [^{3}H]-YM-09151-2 vs. increasing concentrations of free competitors NE, DA, and RX821002 (**a**) and of D_1-like receptor antagonist [^{3}H]SCH 23390 vs. increasing concentrations of DA and NE (**b**) in the sheep brain striatum. Values are expressed as a percentage of the specific binding (100% is 0.13 ± 0.01 pmol/mg protein in **a** and 0.43 ± 0.04 pmol/mg protein in **b**). Experimental data were fitted to the two-state dimer receptor model equations, as described in the "Materials and Methods" section. Values are mean ± SEM from a representative experiment (n = 3–5) performed in triplicate

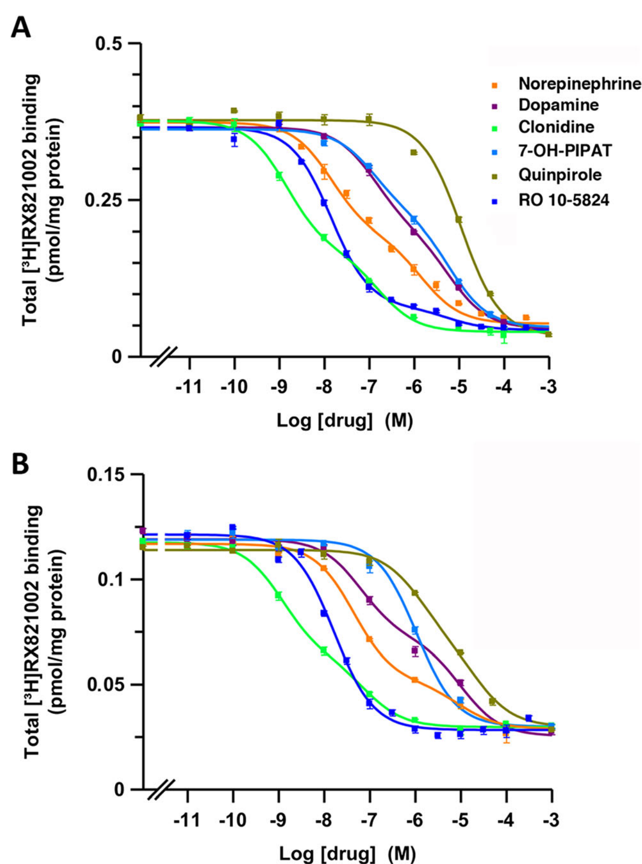

Fig. 2 Radioligand binding of dopaminergic and adrenergic ligands to α_2-adrenoceptors in brain tissue. Representative competition curves of α_2-adrenoceptor antagonist [^{3}H]RX821002 vs. increasing concentrations of free competitors (NE, DA, clonidine, quinpirole, 7-OH-PIPAT, and RO-105824) in sheep brain cortical (**a**) and striatal (**b**) membranes. Experimental data were fitted to the two-state dimer receptor model equations, as described in the "Materials and Methods" section. Values are mean ± SEM from a representative experiment (n = 3) performed in triplicate

cortex, and it was almost ten times lower than the cortical K_{DB2} value (Table 1). Quinpirole also showed differences in the binding parameters between the cortex and striatum, such as a lower K_{DB1} value but negative cooperativity in the striatum. Finally, RO-105824 also displaced [^{3}H]RX821002 binding from the cortex and striatum with high affinity (subnanomolar). No cooperativity (D_{CB} = 0) was obtained, except for RO-105824 in the cortex (D_{CB} = −4.3) (Table 1).

Binding of DA and NE to D_1-Like and D_2-Like Receptors in Striatal Tissue

Next, we compared the affinity of endogenous DA and NE binding to DA D_1-like and D_2-like receptors with the affinity, determined above, for α_2-adrenoceptors. In addition to competition experiments with the D_2-like radioligand antagonist [^{3}H]YM-09151-2 (Fig. 1a), we performed competition experiments with the D_1-like radioligand antagonist [^{3}H]SCH 23390 in sheep striatal preparations (Fig. 1b). The equilibrium binding parameters are shown in Table 2. Both NE and DA showed negative cooperativity (Fig. 1) with negative D_c values (Table 2). The affinity of DA for the first protomer of the D_2-like receptor dimer (K_{DB1}), mostly represented by the D_2R subtype in the dorsal striatum [35], was similar to the affinity for α_2-adrenoceptors and D_1-like receptors (Fig. 1, Table 2). The affinity of DA for the second protomer (K_{DB2}) of the D_1-like receptor was even about ten times lower than that for the α_2-adrenoceptors and D_2-like receptors (stronger negative cooperativity; see Table 2). On the other hand, the affinity of NE for α_2-adrenoceptors in the striatum, represented by α_{2A}- and α_{2C}-adrenoceptors, was significantly higher than that for dopamine receptors (Fig. 1). Specifically, NE had an affinity for DA receptors about 60-fold lower than that for α_2-adrenoceptors (Table 2, Fig. 1). We can therefore assume that extracellular physiological levels of DA that are

Table 1 Competitive inhibition experiments of [^{3}H]RX821002 versus NE, DA, clonidine, and D_2-like receptor ligands in the sheep brain cortex and striatum

Ligand	Binding parameters	
	Cortex	Striatum
NE	$K_{DB1} = 0.3 \pm 0.2$*	$K_{DB1} = 0.8 \pm 0.1$
	$K_{DB2} = 250 \pm 100$	$K_{DB2} = 5000 \pm 3000$
	$D_{CB} = -2.3$	$D_{CB} = -3.2$
DA	$K_{DB1} = 6.9 \pm 0.2$	$K_{DB1} = 6 \pm 1$
	$K_{DB2} = 350 \pm 10$*	$K_{DB2} = 1000 \pm 200$
	$D_{CB} = -1.1$	$D_{CB} = -1.6$
Clonidine	$K_{DB1} = 0.014 \pm 0.003$*	$K_{DB1} = 0.036 \pm 0.005$
	$K_{DB2} = 40 \pm 20$	$K_{DB2} = 20 \pm 10$
	$D_{CB} = -2.8$	$D_{CB} = -2.1$
7-OH-PIPAT	$K_{DB1} = 9 \pm 2$**	$K_{DB1} = 51 \pm 6$
	$K_{DB2} = 430 \pm 80$	
	$D_{CB} = -1.1$	$D_{CB} = 0$
Quinpirole	$K_{DB1} = 530 \pm 50$**	$K_{DB1} = 110 \pm 10$
		$K_{DB2} = 2700 \pm 400$
	$D_{CB} = 0$	$D_{CB} = -0.8$
RO-105824	$K_{DB1} = 0.055 \pm 0.003$***	$K_{DB1} = 0.42 \pm 0.03$
	$K_{DB2} = 4000 \pm 2000$	
	$D_{CB} = -4.3$	$D_{CB} = 0$

Binding parameters from competitive inhibition experiments of [^{3}H]RX821002 versus NE, DA, clonidine, and D_2-like receptor ligands in membrane preparations from the sheep brain cortex and striatum (Fig. 2). K_{DB1}, K_{DB2}, and D_{CB} values were obtained according to the two-state dimer model (see "Materials and Methods" and ref. 22). K_{DB1} and K_{DB2} (in nM) are expressed as means ± SEM of three experiments performed in triplicate. Statistical differences between affinity parameters of cortical versus striatal adrenoceptors were calculated by non-paired, two-tailed Student's t test

*$p < 0.05$; **$p < 0.01$; ***$p < 0.001$

Table 2 Competitive inhibition experiments of [^{3}H]SCH 23390, [^{3}H]YM-09151-2, or [^{3}H]RX821002 versus DA and NE in the sheep brain striatum

Receptor	Binding parameters	
	DA	NE
D_1-like	$K_{DB1} = 8 \pm 3$	$K_{DB1} = 53 \pm 90^{\#\#}$
	$K_{DB2} = 8000 \pm 1000$***	$K_{DB2} = 50000 \pm 10{,}000^{\#}$
	$D_c = -2.4$	$D_c = -2.4$
D_2-like	$K_{DB1} = 3.5 \pm 0.6$	$K_{DB1} = 60 \pm 40^{\#\#}$
	$K_{DB2} = 700 \pm 200$	$K_{DB2} = 3400 \pm 100$
	$D_c = -1.7$	$D_c = -1.2$
α_2	$K_{DB1} = 6 \pm 1$	$K_{DB1} = 0.8 \pm 0.1$
	$K_{DB2} = 1000 \pm 200$	$K_{DB2} = 5000 \pm 3000$
	$D_c = -1.6$	$D_c = -3.2$

Binding parameters from competitive inhibition experiments of [^{3}H]SCH 23390 (D_1-like receptor antagonist), [^{3}H]YM-09151-2 (D_2-like receptor antagonist), or [^{3}H]RX821002 (α_2 receptor antagonist) versus NE and DA in the sheep brain striatum. K_{DB1}, K_{DB2}, and D_c values were obtained according to the two-state dimer model (see "Materials and Methods" and ref. 22). Values for α_2-adrenoceptors are from Table 1. K_{DB1} and K_{DB2} (in nM) are expressed as means ± SEM of three to five experiments performed in triplicate. Statistical differences between affinity parameters obtained were calculated by one-way ANOVA followed by Dunnett's post hoc test

For DA, ***$p < 0.001$ vs. D_2-like receptors; for NE, $^{\#}p < 0.05$ and $^{\#\#}p < 0.01$ vs. α_2 receptors

able to activate DA receptors are also able to bind α_2-adrenoceptors.

α_{2A}- and α_{2C}-Adrenoceptor-Mediated G Protein Activation by DA and Synthetic DA Receptor Ligands

The G protein activation BRET assay (see "Materials and Methods") was used to determine the potency and efficacy of the above-studied ligands to activate α-adrenoceptors in HEK-293T cells transfected with α_{2A}- or α_{2C}-adrenoceptor and one of the five different RLuc-fused Gαi/o subunits (Gαi1, Gαi2, Gαi3, Gαo1, and Gαo2) with Venus-fused Gγ2 protein as BRET acceptor pair. The amount of Gαi/o subunits transfected produced values between 0.5 and 1 million luminescence units (arbitrary units). Previously, we found that luminescence values between 200,000 and 1.5 million did not produce a significant alteration of the E_{max} of drug-induced BRET. Moreover, the levels of α_2-adrenoceptor were around 2 pmol/mg protein. We also previously reported that, using the same cell line and assay conditions, neither DA or NE produces a significant BRET change when transfected with the same fused G protein subunits but without receptor co-transfection [19]. These transfected receptor levels were only slightly higher than those obtained in binding experiments in the sheep brain cortex (see above). A concentration response of the ligand-induced change in BRET values allows to determine the potency as well as the relative efficacy (to NE) at α_{2A}- and α_{2C}-adrenoceptor-mediated G protein activation. Results were largely in agreement with the values obtained with binding experiments, considering that cortical values should represent ligand binding parameters of α_{2A}-adrenoceptors, while striatal values represent combined ligand binding parameters for both α_{2A}- and α_{2C}-adrenoceptors. NE was more potent at α_{2A}- than at α_{2C}-adrenoceptor, except for Gαi2 and Gαi3. On the other hand, DA had similar potencies at both adrenoceptors, except for Gαi2 and Gαo1. At both α_{2A}- and α_{2C}-adrenoceptors, DA showed high potency and efficacy as compared with NE (Figs. 3 and 4, Tables 3 and 4), although DA was always less potent than NE. The relative DA/NE potency depended on the α-adrenoceptor and on the Gαi/o subtype (see Table 3). Therefore, the potencies of DA at activating α_{2A}-adrenoceptor varied from about 15-fold lower, for Gαi1, to about 30-fold lower, for Gαo1. On the other hand, the potencies of DA as compared to NE at activating α_{2C}-adrenoceptor were

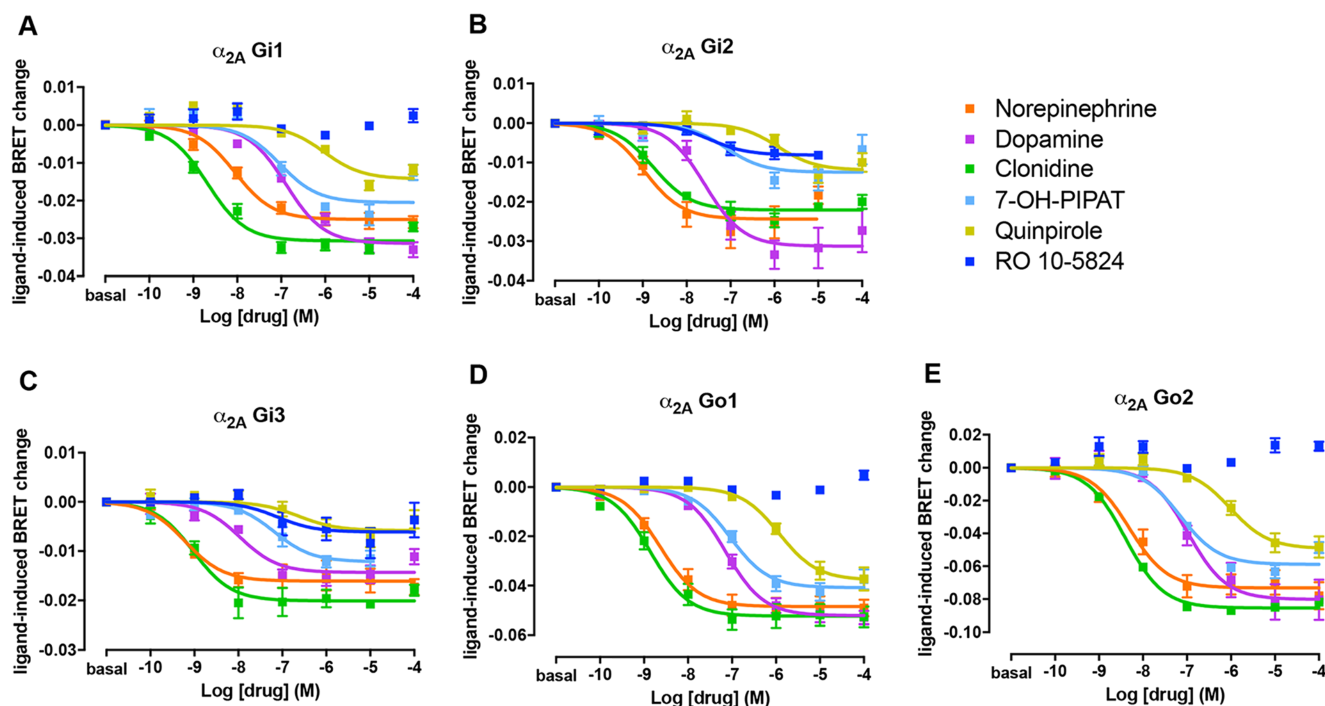

Fig. 3 G protein activation of α_{2A} by dopaminergic and adrenergic ligands. Concentration-response experiments of G protein activation by NE, DA, clonidine, and D_2-like receptor ligands mediated by α_{2A} in HEK-293T cells transiently transfected with α_{2A}-adrenoceptor; the G protein subunits Gαi1-RLuc (**a**), Gαi2-RLuc (**b**), Gαi3-RLuc (**c**), Gαo1-Rluc (**d**), or Gαo2-RLuc (**e**); γ2-mVenus, and non-fused β1. Cells were treated with coelenterazine H followed by increasing concentrations of one of the ligands. Ligand-induced changes in BRET values were measured as described in the "Materials and Methods" section. BRET values in the absence of ligands were subtracted from the BRET values for each agonist concentration. Data were adjusted to a sigmoidal concentration-response function by non-linear regression analysis and represent means ± SEM of 3 to 11 experiments performed in triplicate (see Tables 1 and 2 for EC_{50} and E_{max} values and statistical analysis)

very close to those of NE and they varied from less than twofold lower, for Gαi1, to about 70-fold lower, for Gαi3 (Table 3).

The prototypical non-selective α-adrenoceptor agonist clonidine only showed a significantly higher potency at α_{2A}- than at α_{2C}-adrenoceptors for Gαo1 and Gαo2 (Table 3). An additional difference as compared to NE was that clonidine behaved as a full agonist at α_{2A}- and as a partial agonist at α_{2C}-adrenoceptor, except for Gαi2 and Gαi3 (Figs. 3 and 4, Table 4). Intriguingly, the level of efficacy of clonidine for α_{2C}-adrenoceptor varied significantly with the associated Gαi/o protein subtypes, from no decrease for Gαi2 to a very significant loss of efficacy for Gαo1 (Table 4). Previous studies have already reported a partial agonism of clonidine at α_2-adrenoceptors, but with disparate results [36, 37], which, at least for α_{2C}, could be related to the Gαi/o protein subtypes involved. In summary, the differences in the respective potency values of NE, clonidine, and DA for α_{2A}- and α_{2C}-adrenoceptors in the G protein activation BRET experiments correlate with the higher affinities of NE and clonidine in the cortex and similar affinities of DA in the cortex and striatum.

The non-selective D_2-D_3-D_4 receptor agonist quinpirole and the selective D_3 receptor agonist 7-OH-PIPAT also activated α_{2A}- and α_{2C}-adrenoceptors, but with very different profiles (see Figs. 3 and 4, Tables 3 and 4). 7-OH-PIPAT behaved as a low efficacious agonist at α_{2A}-adrenoceptors for the Gαi2 subtype. On the other hand, 7-OH-PIPAT behaved as a partial agonist at α_{2C}-Gαi1 complexes but as a full agonist with the other α_{2C}-Gαi/o complexes. This D_3 receptor agonist, at α_{2A}-adrenoceptor, was, in general, as potent as DA and, for both Gαo subtypes, was as potent α_{2C}-adrenoceptor agonist as NE. In contrast, quinpirole showed a weak potency (submicromolar range) but also behaved as a partial or full agonist depending on the Gαi/o subtype. At α_{2A}, quinpirole behaved as a partial agonist for Gi1, Gi2, and Gi3 and a full agonist for Go1 and Go2, whereas at α_{2C}, it behaved as a partial agonist for all G protein subtypes except for Gi3 (full agonist) and showed no activity when coupled with Gαi1. As shown in Fig. 5, yohimbine, a non-selective α_2-adrenoceptor antagonist, completely blocked the effect of 7-OH-PIPAT and quinpirole at both α_{2A}- and α_{2C}-adrenoceptors (for Gαo1), demonstrating the specificity of the α_2-adrenoceptor signal produced by both agonists. The potency values of 7-OH-PIPAT and quinpirole in G protein activation BRET experiments correlate with the nanomolar and submicromolar affinities, respectively, as seen in binding assays with brain membranes. Moreover, the higher potencies of 7-OH-PIPAT for α_{2C}- versus α_{2A}-adrenoceptors also correlate with our binding results due to the fact that 7-OH-PIPAT showed negative

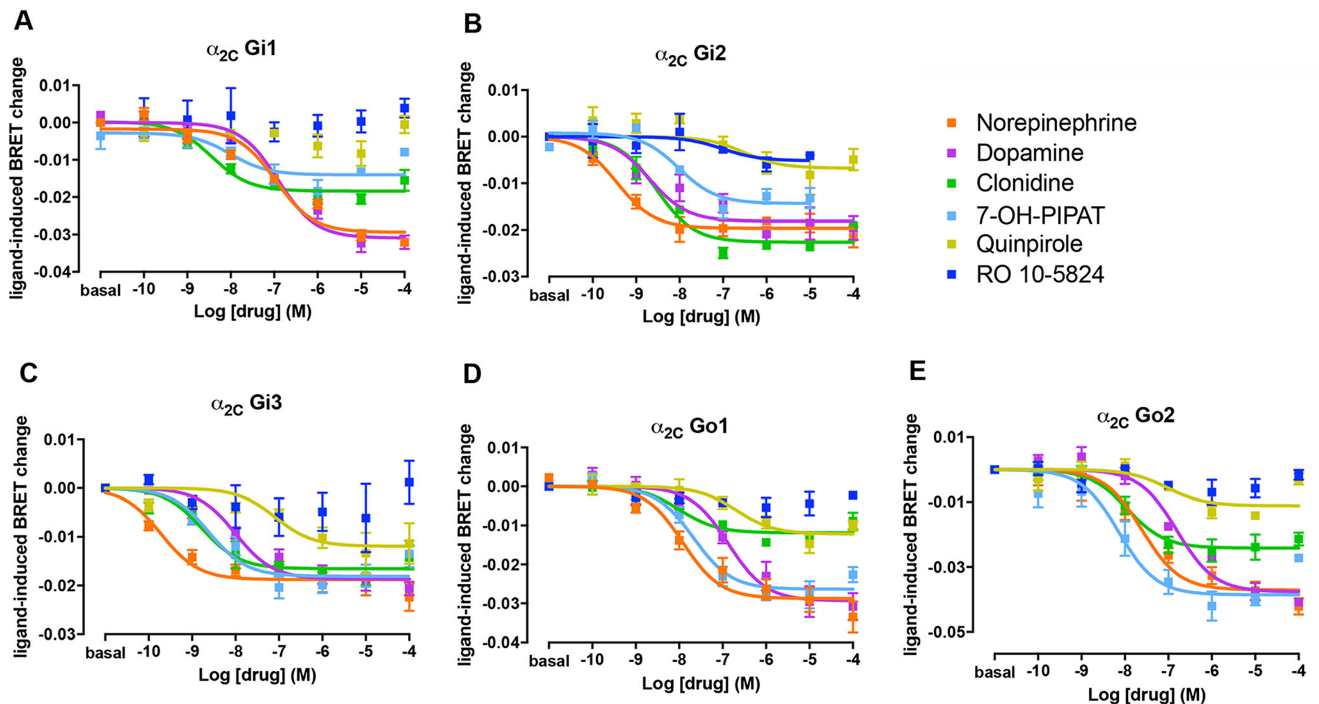

Fig. 4 G protein activation of α_{2C} by dopaminergic and adrenergic ligands. Concentration-response experiments of G protein activation by NE, DA, clonidine, and D_2-like receptor ligands mediated by α_{2C} in HEK-293T cells transiently transfected with α_{2C} receptor; the G protein subunits Gαi1-RLuc (**a**), Gαi2-RLuc (**b**), Gαi3-RLuc (**c**), Gαo1-RLuc (**d**), or Gαo2-RLuc (**e**), γ2-mVenus; and non-fused β1. Cells were treated with coelenterazine H followed by increasing concentrations of one of the ligands. Ligand-induced changes in BRET values were measured as described in the "Materials and Methods" section. BRET values in the absence of ligands were subtracted from the BRET values for each agonist concentration. Data were adjusted to a sigmoidal concentration-response function by non-linear regression analysis and represent means ± SEM of three to nine experiments performed in triplicate (see Tables 1 and 2 for EC_{50} and E_{max} values and statistical analysis)

cooperativity in the cortex but not in the striatum. For quinpirole, however, it would be difficult to establish correlations with results from binding assays due to its low efficacy in BRET assays, which might lead to inaccurate values (Table 3, in parentheses, and Table 4, in italics). Finally, and unexpectedly, the selective D_4 receptor agonist RO-105824 (with

Table 3 Potency of NE, DA, clonidine, 7-OH-PIPAT, and quinpirole obtained from G protein activation experiments mediated by α_{2A}- and α_{2C}-adrenoceptors coupled to the different Gαi/o subtypes

Gα subunit	Receptor	NE	DA	Clonidine	7-OH-PIPAT	Quinpirole	DA/NE[a]
Gαi1	α_{2A}	11 ± 2**	170 ± 40	3 ± 1	80 ± 20*	700 ± 250	15
	α_{2C}	90 ± 30	150 ± 40	6 ± 2	(11 ± 4)	ND	1.7
Gαi2	α_{2A}	1.3 ± 0.3*	30 ± 3**	2.0 ± 0.8	120 ± 6*	(1000 ± 300)	23
	α_{2C}	0.4 ± 0.2	5 ± 3	3 ± 1	10 ± 2	(200 ± 100)	12.5
Gαi3	α_{2A}	0.6 ± 0.2	15 ± 5	1.0 ± 0.2	60 ± 20*	(700 ± 400)	25
	α_{2C}	0.4 ± 0.2	30 ± 20	4 ± 1	5 ± 3	400 ± 100	75
Gαo1	α_{2A}	3.0 ± 0.5*	80 ± 10**	2.0 ± 0.4*	100 ± 20**	1300 ± 200**	27
	α_{2C}	19 ± 6	126 ± 8	(12 ± 5)	20 ± 3	(230 ± 50)	7
Gαo2	α_{2A}	6 ± 1*	100 ± 20	4.0 ± 0.2**	66 ± 7*	820 ± 80***	17
	α_{2C}	50 ± 10	140 ± 20	11 ± 2	14 ± 7	(100 ± 10)	2.8

Potency (EC_{50} values, in nM) of NE, DA, clonidine, and D_2-like receptor ligands obtained from G protein activation experiments mediated by α_{2A} and α_{2C} coupled to the different Gαi/o subtypes (Figs. 3 and 4). EC_{50} values were obtained from a sigmoidal concentration-response function adjusted by non-linear regression analysis and are expressed as means ± SEM of 3 to 11 experiments performed in triplicate. In parentheses, values corresponding to experiments show low efficacy, E_{max} lower than 50% (Table 4). Statistical differences between α_{2A}- and α_{2C}-adrenoceptors were calculated by non-paired, two-tailed Student's *t* test

*$p < 0.05$; **$p < 0.01$; ***$p < 0.001$

[a] The ratio of EC_{50} values of DA and NE for each receptor and Gαi/o protein subtype

Table 4 Efficacy of NE, DA, clonidine, 7-OH-PIPAT, and quinpirole obtained from G protein activation experiments mediated by α_{2A}- and α_{2C}-adrenoceptors coupled to the different Gαi/o subtypes

Gα subunit	Receptor	NE	DA	Clonidine	7-OH-PIPAT	Quinpirole
Gαi1	α_{2A}	100 ± 5	120 ± 6*	120 ± 5	94 ± 6	70 ± 2*
	α_{2C}	100 ± 2	105 ± 5	64 ± 4**	*41 ± 1***	ND
Gαi2	α_{2A}	100 ± 10	120 ± 20	89 ± 6	55 ± 2*	*47 ± 8**
	α_{2C}	100 ± 7	80 ± 10	107 ± 4	90 ± 20	*46 ± 9***
Gαi3	α_{2A}	100 ± 10	90 ± 10	112 ± 8	71 ± 6	*40 ± 9***
	α_{2C}	100 ± 9	95 ± 6	85 ± 5	90 ± 10	80 ± 15
Gαo1	α_{2A}	100 ± 7	108 ± 6	110 ± 10	81 ± 9	78 ± 9
	α_{2C}	100 ± 10	100 ± 10	*41 ± 3***	98 ± 7	*42 ± 3***
Gαo2	α_{2A}	100 ± 9	110 ± 10	120 ± 2	85 ± 4	72 ± 8
	α_{2C}	100 ± 8	114 ± 6	70 ± 8*	106 ± 3	*34 ± 6***

Efficacy (E_{max} values, as the percentage of NE values) of NE, DA, clonidine, and D_2-like receptor ligands obtained from G protein activation experiments mediated by α_{2A} and α_{2C} coupled to the different Gαi/o subtypes (Figs. 3 and 4). E_{max} values were obtained from a sigmoidal concentration-response function adjusted by non-linear regression analysis and are expressed as means ± SEM of 3 to 11 experiments performed in triplicate. In italics, values of E_{max} are lower than 50%. Statistical differences between NE and the other ligands for each receptor and Gαi/o protein subtype were calculated by one-way ANOVA, followed by Dunnett's post hoc test

ND not detectable

*$p < 0.05$; **$p < 0.01$; ***$p < 0.001$

subnanomolar affinity for α-adrenoceptors) did not produce a significant activation of α_{2A}- or α_{2C}-adrenoceptors coupled to any of the Gαi/o subtypes, except for a small efficacy at α_{2A} for Gαi2 and Gαi3 (Figs. 3 and 4). To confirm the binding of this putative selective D_4 receptor ligand to α_{2A}- and α_{2C}-adrenoceptors, they were tested for their ability to modify the effect of clonidine. RO-105824 did counteract the respective full and partial agonistic effect of clonidine (1 μM) at the α_{2A}- and α_{2C}-adrenoceptors coupled to Gαo1 (Fig. 5c, d). Therefore, the results of BRET and radioligand binding experiments disclosed a previously unknown additional role of the D_4 receptor agonist RO-105824, as a very potent and low-efficacious ligand for α_2-adrenoceptors at Gαi/o activation.

We also determined the effect of DA and synthetic DA receptor ligands on a DMR label-free assay in CHO-transfected cells. This approach detects changes in local optical density due to cellular mass movements induced upon receptor activation (see the "Materials and Methods" section), and DMR responses primarily reflect G protein-dependent signaling in living cells, since it can be abrogated by toxins or inhibitors of the G proteins involved [38]. DA was as capable as NE at activating cellular signaling in CHO cells transfected with α_{2A}-RLuc8 receptor (Fig. 6a). The amount of α_{2A}-RLuc8 receptor expressed was about 0.3 pmol/mg protein. DA and NE activation decreased by adding the α_{2A}R-antagonist BRL 44408, indicating the specificity of the cell activation through α_{2A}-receptor. The synthetic DA receptor ligands 7-OH-PIPAT, quinpirole, and RO-105824 at 300 nM were also able to produce a significant response (Fig. 6b), substantially lower for RO-105824, which correlates with the G protein activation BRET assays (Fig. 3). These results indicate that DA and synthetic DA receptor ligands are also α_2-adrenoceptor ligands able to activate Gαi/o proteins, which correlate with their efficacy with DMR.

α_{2A}- and α_{2C}-Adrenoceptor-Mediated Effects of NE and DA on Adenylyl Cyclase Activity

NE- and DA-induced changes in adenylyl cyclase activity were also analyzed by measuring cAMP levels in intact cells transiently transfected with α_{2A}- or α_{2C}-adrenoceptor, using the CAMYEL BRET biosensor (see the "Materials and Methods" section and ref. 21). HEK-293T cells have been reported to endogenously express β-adrenoceptors [39]. Accordingly, we recently reported that NE, in non-transfected HEK-293T cells, stimulated a Gs-mediated cAMP increase, which could be completely inhibited by the selective β-adrenergic blocker propranolol (10 μM) (ref. 19; the same website address as above). Therefore, the β-adrenoceptor antagonist propranolol was added throughout the cAMP detection experiments. As shown in Fig. 7, NE and DA produced an increase in BRET, corresponding to a decrease in forskolin-induced cAMP accumulation for both α_{2A}- and α_{2C}-adrenoceptor-transfected cells. The decrease in adenylyl cyclase activity by NE and DA provided apparent half maximal effective concentration (EC_{50}) values that were qualitatively and quantitatively close to those observed with the Gi/o activation BRET assays, as NE was more potent than DA at α_{2A} and α_{2C} (1.4 ± 0.2 and 7 ± 4 nM for NE and 140 ± 40 and 90 ± 20 nM for DA, respectively). The putative Gi/o-dependent effects mediated by NE and DA were blocked by the non-selective α_2-adrenoceptor antagonist yohimbine, confirming the receptor specificity of the signal (Fig. 7). In

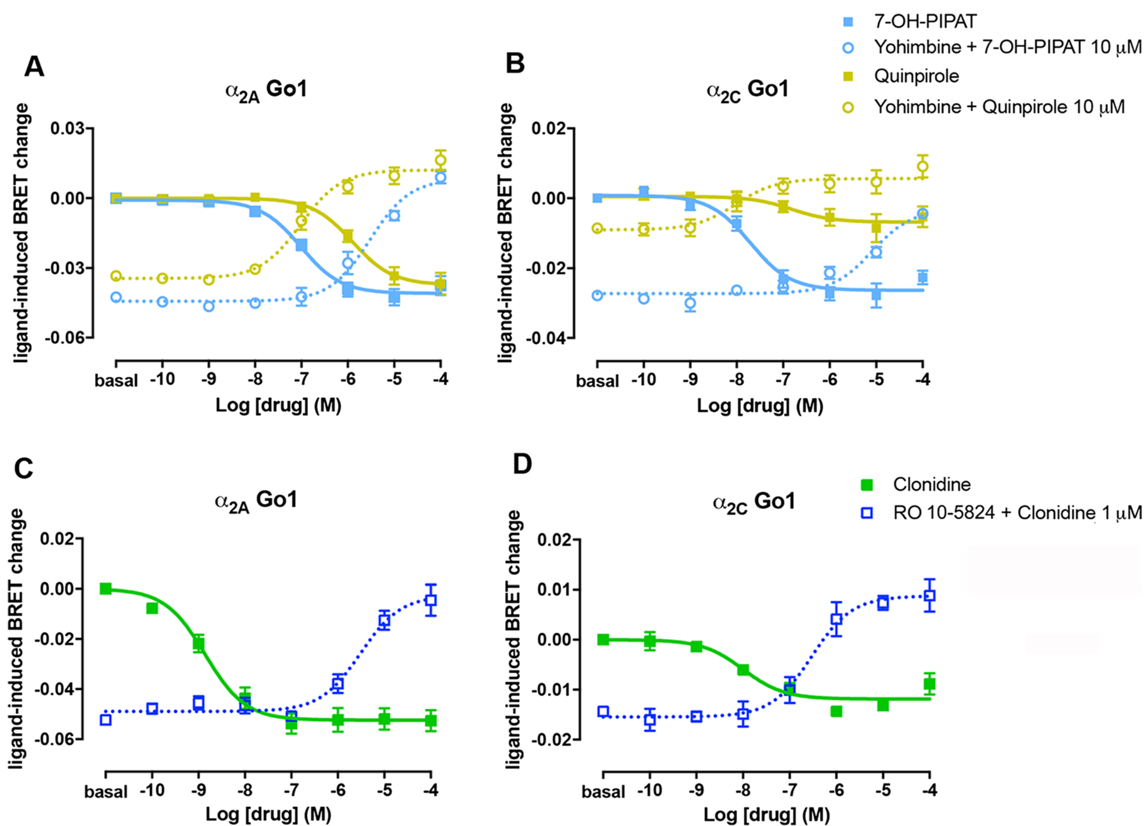

Fig. 5 Specificity of the effect of dopaminergic ligands on α_{2A}- and α_{2C}-adrenoceptors. **a**, **b** Dose-dependent inhibition by increasing concentrations of the non-selective α_2 receptor antagonist yohimbine of Gαo1 protein activation induced by 10 μM of the D$_2$-like receptor agonists 7-OH-PIPAT (dotted blue) or 10 μM of quinpirole (dotted yellow) in HEK-293T cells transfected with α_{2A} (**a**) or α_{2C} (**b**) adrenoceptors, Gαo1-RLuc, γ_2-mVenus, and non-fused β_1. As controls, concentration-response curves of Gαo1 protein activation by 7-OH-PIPAT (full blue) or quinpirole (full yellow) from Figs. 3d and 4d are showed. Cells were treated with coelenterazine H followed by the addition of 7-OH-PIPAT or quinpirole. Ligand-induced changes in BRET values were measured as described in the "Materials and Methods" section. **c**, **d** Dose-dependent inhibition of the agonistic effect of clonidine at 1 μM by increasing concentrations of RO-105824 (dark blue) in cells transfected with α_{2A} (**c**) or α_{2C} (**d**) adrenoceptors, Gαo1-RLuc, γ_2-mVenus, and non-fused β_1. As controls, concentration-response curves of Gαo1 protein activation by clonidine (full green) from Figs. 3d and 4d are showed. Data were adjusted to a sigmoidal concentration-response function by non-linear regression analysis and represent means ± SEM of three to six experiments performed in triplicate

addition, cells were treated with pertussis toxin which catalyzes the ADP ribosylation of the αi subunits of the heterotrimeric G protein, preventing its interaction with the receptor. As expected, pertussis toxin treatment selectively eliminated the initial, therefore Gi-dependent, component of the NE- and DA-mediated effects (Fig. 7). Surprisingly, NE and DA showed inverted U-shaped concentration-response curves with a putative Gs-dependent profile at high ligand concentrations for both α_{2A}- and α_{2C}-adrenoceptor-transfected cells (Fig. 7). These results could be explained by considering previous studies showing that α_2-adrenoceptors functionally couple not only to Gi/o proteins but also to Gs [40–44]. Typically, the agonist concentrations necessary to elicit detectable stimulation of adenylyl cyclase are significantly higher than those for inhibition. Equivocal results were published by Zhang et al. [16] when comparing the effect of NE and DA on forskolin-induced adenylyl cyclase activation. In their cell systems, NE seemed to predominantly activate Gs with α_{2A} and Gi with α_{2C}, while DA would predominantly activate Gi with both receptors, but at high micromolar concentrations. In contrast, our experiments show that NE and DA follow the same differential concentration-dependent effects on Gi/o and Gs activation and, at least, at 10 and 100 μM, DA and NE promoted Gs activation mediated by both α_{2A}- and α_{2C}-adrenoceptors (Fig. 7).

α_{2A}- and α_{2C}-Adrenoceptor-Mediated Effects of NE, DA, and Synthetic DA Receptor Ligands on ERK1/2 Phosphorylation

Finally, we studied the ability of DA and synthetic DA receptor ligands to produce MAPK activation. First, we analyzed the increase on ERK1/2 phosphorylation produced by 300 nM of NE in CHO cells transfected with α_{2A}-RLuc8 receptor. This NE concentration increased ERK1/2 phosphorylation levels by threefold over basal, and this effect was similar to that produced by 1 μM of DA (Fig. 8). Next, we demonstrated that the synthetic DA receptor ligands 7-OH-PIPAT, quinpirole, and RO-105824, at 1 μM, were also able to

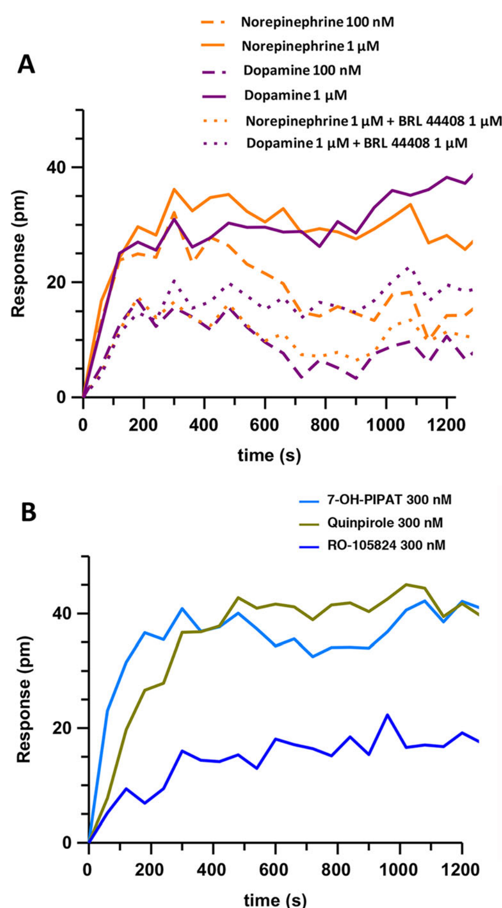

Fig. 6 DMR induced by NE, DA, and synthetic DA receptor ligands using label-free assay. DMR assay was performed in CHO cells transfected with α_{2A}-adrenoceptor. **a** Cells were pretreated (dotted lines) or not (full lines) with the α_{2A}-adrenoceptor antagonist BRL 44408 at 1 μM for 30 min before adding the endogenous agonists DA or NE at 300 nM or 1 μM. **b** Cells were treated with 100 nM of several synthetic DA receptor ligands. The resulting shifts of reflected light wavelength (pm) were monitored over time. Each panel is a representative experiment of $n = 3$ different experiments. Each curve is the mean of a representative optical trace experiment carried out in triplicates

produce MAPK activation (Fig. 8). At this concentration, the efficacy of RO-105824 was similar to that of the other ligands. Together with its very low efficacy disclosed on G protein activation and DMR assays, these results indicate that RO-105824 is a biased agonist of α_{2A}-adrenoceptors with functional selectivity for G protein-independent signaling. In summary, adenylyl cyclase activity and ERK1/2 phosphorylation experiments confirm the results from radioligand binding and G protein activation assays, indicating that DA and synthetic DA receptor ligands are efficacious α_2-adrenoceptor agonists.

Structural Basis for DA at α_{2A}- and α_{2C}-Adrenoceptors

An examination of the binding mode of DA to the adrenoceptors was undertaken to model the activity seen in the biological assays. To generate models of α_{2A}- and α_{2C}-adrenoceptors, we used the RosettaCM [25] application within the Rosetta suite of macromolecular modeling tools [26, 45]. This method relies on the optimal alignment of a target sequence with multiple template structures obtained from the PDB which are hybridized together to generate novel models. We submitted the sequence of α_{2A} and α_{2C} to BLAST-P and found the top five crystal templates by sequence identity to be the DA D_3 receptor [27], β_1-adrenoceptor [28], β_2-adrenoceptor [29], serotonin 5-HT_{1B} receptor [30], and serotonin 5-HT_{2B} receptor [31]. Interestingly, the α_2-adrenoceptors have more sequence identity in the transmembrane helical bundle with the D_3 receptor than with the related β-adrenoceptors. RosettaCM yielded an ensemble of low-energy models of the receptors, which were clustered by structural similarity. The top five cluster centers were included in the docking studies to account for structural diversity and uncertainty in homology modeling. To understand DA activation, we first examined the binding of DA to the D_3 receptor, the only crystal structure of a DA receptor to date. As there is not a co-crystal structure of DA/D_3 receptor, we first docked DA to the D_3 receptor using RosettaLigand [33]. The starting coordinates of epinephrine bound to the β_2-adrenoceptor [46] were used to place DA for docking. Binding pocket analysis identified residue D3.32 interacting with the primary amine in DA and the catechol hydroxyls interacting with S5.42 and S5.46. Important hydrophobic packing against the central portion of DA was achieved by V3.33, H6.55, and F6.51. These are the same interactions that were previously identified in a molecular dynamics simulation of DA binding at D_3 receptor [47]. Comparing the residues at these positions to those in α_{2A}- and α_{2C}-adrenoceptors revealed identity at all residues except position 6.55, in which the His has been replaced with a Tyr in both α_{2A}- and α_{2C}-adrenoceptors. Docking results of DA at either α_{2A} or α_{2C} also identified many of these same residues as critical for binding. Particularly, D3.32, V3.33, S5.42, and F6.51 were present in all receptor models contributing more than − 0.4 Rosetta energy units each to the binding of DA (Fig. 9). Residues S5.46 and Y6.55 were also present in all receptor binding modes though contributions varied depending on which receptor type. These results coupled with those from the biological assays provide a strong structural reasoning behind the activity of DA at the α_{2A}- or α_{2C}-adrenoceptors.

Discussion

Previous studies reported DA as a potential α_2-adrenoceptor ligand on the basis of radioligand binding experiments in transfected mammalian and insect cell lines [16, 17] and in bird and rat brains [18] and also from autoradiographic experiments in tissues [18]. Furthermore, DA has been reported to decrease cAMP intracellular levels in transfected mammalian

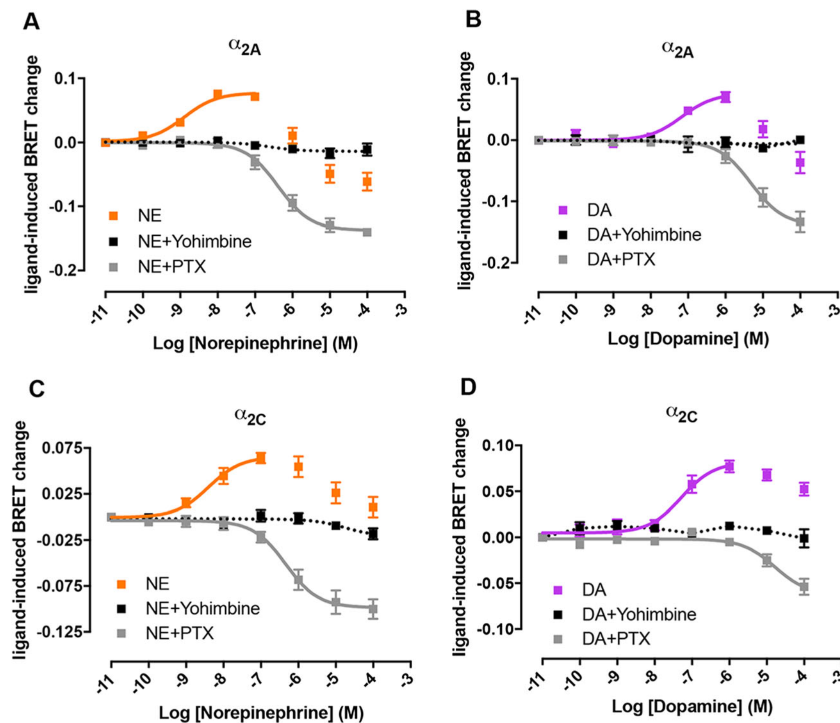

Fig. 7 Effect of NE and DA on the modulation of adenylyl cyclase activity by activation of α_{2A}- and α_{2C}-adrenoceptors. Concentration-response experiments of inhibition of forskolin-induced adenylyl cyclase activity by NE (orange) or DA (purple) mediated by α_{2A} (**a**, **b**) or α_{2C}-adrenoceptors (**c**, **d**) in HEK-293T cells transiently transfected with the CAMYEL sensor and one of the receptors. Cells were treated with forskolin (1 μM) for 10 min with or without the selective α_2 antagonist yohimbine (10 μM) followed by the addition of coelenterazine H and increasing concentrations of NE or DA. After 10 min, BRET was measured as described in the "Materials and Methods" section. In gray, cells were treated with 100 ng/ml pertussis toxin (PTX) for 16–18 h previous to the experiment. Values obtained with forskolin alone were subtracted from BRET values for each agonist concentration. Data represent the mean ± SEM of three to seven experiments performed in triplicate

cell lines but only throughout α_{2C}-adrenoceptors, not α_{2A}-adrenoceptors, and at concentrations much higher than NE (EC_{50} in the micromolar range) [18].

In our study, we show that α_{2A}- and α_{2C}-adrenoceptors can bind DA at concentrations in the same order than NE, suggesting that they could be activated by DA at in vivo concentrations. First, our results demonstrate that endogenous DA, and also common synthetic DA receptor ligands, binds to α_2-adrenoceptors with moderate to high affinity in the mammalian brain. Second, the affinity of DA for α_2-adrenoceptors is in the same range as for D_1-like and D_2-like receptors, suggesting that endogenous

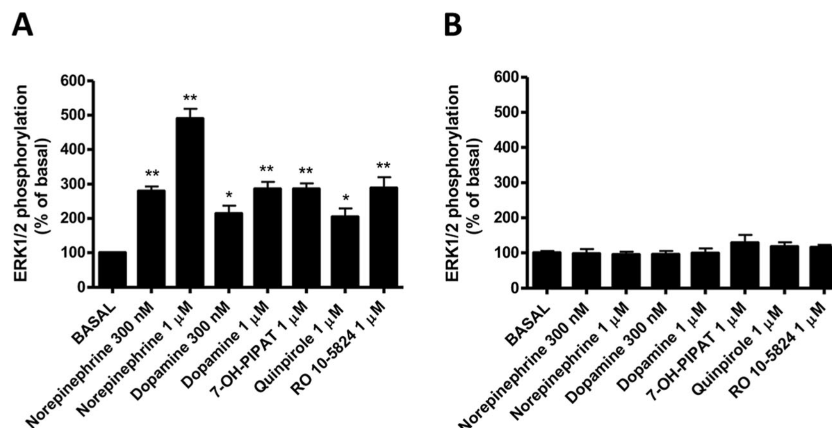

Fig. 8 NE, DA, and synthetic DA receptor ligands signaling via ERK1/2 phosphorylation. ERK1/2 phosphorylation was determined in CHO cells transfected with the α_{2A}-adrenoceptor (**a**) and non-transfected control cells (**b**), treated with 300 nM or 1 μM of the tested ligands for 5 min at 37 °C. Values are expressed as mean ± SEM (n = 6) of percentage of phosphorylation relative to basal levels in non-treated cells. Statistical differences vs. basal conditions were calculated by one-way ANOVA followed by Dunnett's post hoc test; $*p < 0.05$ and $**p < 0.01$

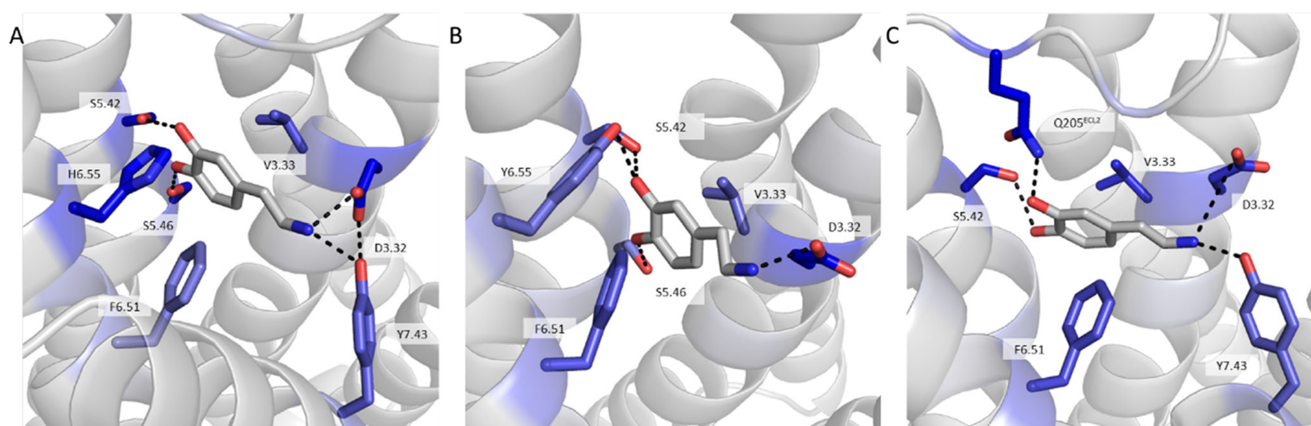

Fig. 9 Binding mode of DA at each receptor type. Shown is the docking orientation of DA at the D_3 receptor (**a**), α_{2A}-adrenoceptor (**b**), and α_{2C}-adrenoceptor (**c**). Residues were scored for binding energy ΔΔG, and those most strongly contributing to the binding of DA are shown in stick representation. The strength of binding interaction is colored by the depth of blue with dark blue being the most strongly contributing. Important hydrogen bonds to the amine group and catechol hydroxyls are formed in all binding poses

levels of DA can activate both α_2-adrenoceptors and dopamine receptors. Third, DA and synthetic DA receptor ligands can activate G protein and induce cell DMR through α_2-adrenoceptors. Finally, DA and NE show the same cell signaling pattern, being both capable to modulate adenylyl cyclase activity and ERK1/2 phosphorylation at nanomolar concentrations.

The most conclusive demonstration that DA is an α_2-adrenoceptor ligand comes from the results obtained with binding and G protein activation BRET assays, where the affinities or potencies of DA for α_2-adrenoceptors were found to be very similar or even higher than for D_1-like and some subtypes of D_2-like receptors [19]. Particularly, the EC_{50} values of DA for α_{2A}- and α_{2C}-adrenoceptors (5–170 nM) were consistently lower across all Gi/o protein subtypes as compared with the EC_{50} values (130–400 nM) for the predominant striatal D_2-like receptor D_{2L} [19]. Taking into account that the levels of tonic extracellular DA are 20–30 nM (with peaks of 500 nM) [48], DA could reach sufficient extracellular concentration to activate α_{2A}- and α_{2C}-adrenoceptors in the striatum, irrespective of the maximal concentration of extracellular NE. In fact, striatal DA release sites are designed for transmitter spillover [49] and most striatal DA receptors are primarily extrasynaptic [50, 51], as well as striatal adrenoceptors, based on the mismatched low NE innervation [7–11]. Although the specific functional role of the DA-sensitive α_2-adrenoceptors in neuronal striatal function remains to be established, a previous study suggests that they might mediate an inhibitory modulatory role of the Gs/olf-coupled striatal adenosine A_{2A} and DA D_1 receptors [14].

The possibility of DA-mediated activation of α_{2A}- and α_{2C}-adrenoceptors in extrastriatal areas should not, however, be underestimated. Cortical α_{2A}-adrenoceptors are most probably able to be activated by DA, particularly in the prefrontal cortex, which receives a rather dense DA innervation [52]. In fact, there is recent evidence for the localization of α_{2A}-adrenoceptors in the cortical terminals from mesencephalic DA neurons [53], which could play a role as "DA autoreceptors." But, there is also evidence for the localization of both α_{2A}- and α_{2C}-adrenoceptors in the soma and dendrites of the mesencephalic DA cells of both substantia nigra and ventral tegmental areas [53, 54]. Apart from the NE input, these α_{2A}- and α_{2C}-adrenoceptors should be able to act as DA autoreceptors that control the non-synaptic somatodendritic DA release [49]. Adding the present results to our recent study that also indicates a significant role of NE as a Gi/o-coupled D_2-like receptor agonist [19], we could state that Gi/o-coupled adrenoceptors and DA receptors should probably be considered as members of one "functional" family of catecholamine receptors. A general consideration from the DA and D_2-like receptor ligand sensitivity of cortical α_{2A}-adrenoceptors is that it should also be involved in the cognitive-enhancing effects associated with their activation, with possible implications for attention deficit hyperactivity disorder [55].

Molecular modeling of DA binding to the various receptors provides a likely binding hypothesis for the results obtained in the biological assays. Of note is the striking similarity between the ligand binding pocket of the D_3 receptor and that of α_{2A}- and α_{2C}-adrenoceptors. Many of the residues that line the binding pocket are identical or chemically well conserved. Given this similarity, it was perhaps unsurprising that the docking of DA at α_{2A} and α_{2C} was nearly identical to DA binding to the D_3 receptor. The lower potency of DA at α_{2A}- and α_{2C}-adrenoceptors compared to NE seems to depend on a lower number of strong interactions as compared to those between DA and D_3 receptors. The pocket may have evolved to bind the slightly bulkier NE and, therefore, is not of an ideal size for DA. However, the differences may also be due to the lower resolution of binding predictions for a comparative model as opposed to a crystal structure. Despite this, the

structural model strongly mimics the results of the binding and activation experiments and therefore provides further evidence of DA acting as a ligand at these receptors.

Another major finding of the present study is that α_{2A}- and α_{2C}-adrenoceptors are also common targets for compounds previously characterized as D_2-like receptor ligands. Particularly striking was the ability of prototypical D_3 and D_4 receptor agonists 7-OH-PIPAT and RO-105824 to bind with high affinity to α_{2A}- and α_{2C}-adrenoceptors, which might call for revisiting results of previous studies using these compounds. Furthermore, these two compounds and the other DA-synthetic ligands assayed, as well as NE, were able to activate ERK1/2 phosphorylation by binding to α_2-adrenoceptors. The final pharmacological profile of RO-105824 was that of a potent biased agonist for α_{2A}-adrenoceptor with functional selectivity for a G protein-independent signaling. On the other hand, based on BRET experiments, both potency and efficacy dependence on the receptor and the Gαi/o protein subtype were the norm for all ligands, including the endogenous neurotransmitters. We already described that NE and DA show different receptor- and Gαi/o subtype-dependent potencies of D_2-like receptor-mediated G protein activation [19]. The present results extend these findings to other receptors and to non-endogenous ligands, as well as to differences in efficacy. Even though G proteins of the Gαs-Gαolf family do show contrasting brain expression pattern [56], to our knowledge, no clear region-specific pattern of mRNA expression for Gαi/o protein subtypes has been reported. Detailed characterization of the expression patterns for Gαi/o protein subtypes would then be central to determine their role in α_{2A}- and α_{2C}-adrenoceptor activation and thus their possible specific targeting with Gαi/o subtype functionally selective compounds.

In conclusion, DA is a potent and efficacious ligand at α_2-adrenoceptors, which modulates forskolin-induced adenylyl cyclase activity and ERK1/2 phosphorylation. The concentration required for these effects is in the range of that for activating D_2-like and D_1-like receptors, indicating that these receptors are members of one functional family of catecholamine receptors. Our results provide a clear answer to the mismatch between the low striatal NE innervation and the high density of striatal α_2-adrenoceptors, which behave as functional DA receptors.

Acknowledgements The authors would like to thank Dr. Céline Galés (INSERM) for generously sharing various Gi-like plasmid constructs for BRET experiments.

Author Contributions M. S.-S., V. C.-A., H. Y., N.-S. C., E. M., A. C., and B. J. B. performed the experiments and analyzed the data. H. Y., B. J. B., J. M., V. C., and S. F. designed the experiments. M. S.-S., V. C.-A., H. Y., B. J. B., J. M., E. I. C., V. C., and S. F. wrote the manuscript.

Funding Information This research was supported by the "Ministerio de Economía y Competitividad" and European Regional Development Funds of the European Union Grant SAF2014-54840-R, the "Centro de Investigación Biomédica en Red sobre Enfermedades Neurodegenerativas" Grant CB06/05/0064, the "Fundació La Marató de TV3" Grant 20140610, the fellowship from the Japan Society for the Promotion of Science, and intramural funds of the National Institute on Drug Abuse. Work in the Meiler Laboratory is supported through the NIH (R01 GM080403, R01 GM099842, R01 DK097376) and NSF (CHE 1305874).

Compliance with Ethical Standards

Conflict of Interest The authors declare that they have no conflicts of interest.

References

1. Alexander SP, Mathie A, Peters JA (2011) Guide to Receptors and Channels (GRAC), 5th edition. Br J Pharmacol 164(Suppl 1):S1–S324. https://doi.org/10.1111/j.1476-5381.2011.01649_1.x
2. MacDonald E, Kobilka BK, Scheinin M (1997) Gene targeting—homing in on alpha 2-adrenoceptor-subtype function. Trends Pharmacol Sci 18(6):211–219
3. Nicholas AP, Pieribone V, Hokfelt T (1993) Distributions of mRNAs for alpha-2 adrenergic receptor subtypes in rat brain: an in situ hybridization study. J Comp Neurol 328(4):575–594. https://doi.org/10.1002/cne.903280409
4. Scheinin M, Lomasney JW, Hayden-Hixson DM, Schambra UB, Caron MG, Lefkowitz RJ, Fremeau RT Jr (1994) Distribution of alpha 2-adrenergic receptor subtype gene expression in rat brain. Brain Res Mol Brain Res 21(1–2):133–149
5. Fagerholm V, Rokka J, Nyman L, Sallinen J, Tiihonen J, Tupala E, Haaparanta M, Hietala J (2008) Autoradiographic characterization of alpha(2C)-adrenoceptors in the human striatum. Synapse 62(7):508–515. https://doi.org/10.1002/syn.20520
6. Lehto J, Virta JR, Oikonen V, Roivainen A, Luoto P, Arponen E, Helin S, Hietamaki J et al (2015) Test-retest reliability of (11)C-ORM-13070 in PET imaging of alpha2C-adrenoceptors in vivo in the human brain. Eur J Nucl Med Mol Imaging 42(1):120–127. https://doi.org/10.1007/s00259-014-2899-z
7. Ordway GA, Jaconetta SM, Halaris AE (1993) Characterization of subtypes of alpha-2 adrenoceptors in the human brain. J Pharmacol Exp Ther 264(2):967–976
8. Uhlen S, Lindblom J, Tiger G, Wikberg JE (1997) Quantification of alpha2A and alpha2C adrenoceptors in the rat striatum and in different regions of the spinal cord. Acta Physiol Scand 160(4):407–412. https://doi.org/10.1046/j.1365-201X.1997.00175.x
9. Lindvall O, Bjorklund A (1974) The organization of the ascending catecholamine neuron systems in the rat brain as revealed by the glyoxylic acid fluorescence method. Acta Physiol Scand Suppl 412:1–48
10. Swanson LW, Hartman BK (1975) The central adrenergic system. An immunofluorescence study of the location of cell bodies and their efferent connections in the rat utilizing dopamine-beta-hydroxylase as a marker. J Comp Neurol 163(4):467–505. https://doi.org/10.1002/cne.901630406
11. Aston-Jones G (2004) Locus coeruleus, A5 and A7 noradrenergic cell groups. In: Paxinos G (ed) The rat nervous system. Academic, San Diego, pp. 259–294

12. Gobert A, Billiras R, Cistarelli L, Millan MJ (2004) Quantification and pharmacological characterization of dialysate levels of noradrenaline in the striatum of freely-moving rats: release from adrenergic terminals and modulation by alpha2-autoreceptors. J Neurosci Methods 140(1–2):141–152. https://doi.org/10.1016/j.jneumeth.2004.04.040
13. Holmberg M, Scheinin M, Kurose H, Miettinen R (1999) Adrenergic alpha2C-receptors reside in rat striatal GABAergic projection neurons: comparison of radioligand binding and immunohistochemistry. Neuroscience 93(4):1323–1333
14. Hara M, Fukui R, Hieda E, Kuroiwa M, Bateup HS, Kano T, Greengard P, Nishi A (2010) Role of adrenoceptors in the regulation of dopamine/DARPP-32 signaling in neostriatal neurons. J Neurochem 113(4):1046–1059. https://doi.org/10.1111/j.1471-4159.2010.06668.x
15. Ihalainen JA, Tanila H (2004) In vivo regulation of dopamine and noradrenaline release by alpha2A-adrenoceptors in the mouse nucleus accumbens. J Neurochem 91(1):49–56. https://doi.org/10.1111/j.1471-4159.2004.02691.x
16. Zhang W, Klimek V, Farley JT, Zhu MY, Ordway GA (1999) alpha2C adrenoceptors inhibit adenylyl cyclase in mouse striatum: potential activation by dopamine. J Pharmacol Exp Ther 289(3):1286–1292
17. Alachkar A, Brotchie JM, Jones OT (2010) Binding of dopamine and 3-methoxytyramine as l-DOPA metabolites to human alpha(2)-adrenergic and dopaminergic receptors. Neurosci Res 67(3):245–249. https://doi.org/10.1016/j.neures.2010.03.008
18. Cornil CA, Ball GF (2008) Interplay among catecholamine systems: dopamine binds to alpha2-adrenergic receptors in birds and mammals. J Comp Neurol 511(5):610–627. https://doi.org/10.1002/cne.21861
19. Sánchez-Soto M, Bonifazi A, Cai NS, Ellenberger MP, Newman AH, Ferré S, Yano H (2016) Evidence for noncanonical neurotransmitter activation: norepinephrine as a dopamine D2-like receptor agonist. Mol Pharmacol 89(4):457–466. https://doi.org/10.1124/mol.115.101808
20. Urizar E, Yano H, Kolster R, Gales C, Lambert N, Javitch JA (2011) CODA-RET reveals functional selectivity as a result of GPCR heteromerization. Nat Chem Biol 7(9):624–630. https://doi.org/10.1038/nchembio.623
21. Jiang LI, Collins J, Davis R, Lin KM, DeCamp D, Roach T, Hsueh R, Rebres RA et al (2007) Use of a cAMP BRET sensor to characterize a novel regulation of cAMP by the sphingosine 1-phosphate/G13 pathway. J Biol Chem 282(14):10576–10584. https://doi.org/10.1074/jbc.M609695200
22. Casadó V, Cortés A, Ciruela F, Mallol J, Ferré S, Lluis C, Canela EI, Franco R (2007) Old and new ways to calculate the affinity of agonists and antagonists interacting with G-protein-coupled monomeric and dimeric receptors: the receptor-dimer cooperativity index. Pharmacol Ther 116(3):343–354. https://doi.org/10.1016/j.pharmthera.2007.05.010
23. Ferré S, Casadó V, Devi LA, Filizola M, Jockers R, Lohse MJ, Milligan G, Pin JP et al (2014) G protein-coupled receptor oligomerization revisited: functional and pharmacological perspectives. Pharmacol Rev 66(2):413–434. https://doi.org/10.1124/pr.113.008052
24. Casadó V, Ferrada C, Bonaventura J, Gracia E, Mallol J, Canela EI, Lluis C, Cortés A et al (2009) Useful pharmacological parameters for G-protein-coupled receptor homodimers obtained from competition experiments. Agonist-antagonist binding modulation. Biochem Pharmacol 78(12):1456–1463. https://doi.org/10.1016/j.bcp.2009.07.012
25. Song Y, DiMaio F, Wang RY, Kim D, Miles C, Brunette T, Thompson J, Baker D (2013) High-resolution comparative modeling with RosettaCM. Structure 21(10):1735–1742. https://doi.org/10.1016/j.str.2013.08.005
26. Bender BJ, Cisneros A 3rd, Duran AM, Finn JA, Fu D, Lokits AD, Mueller BK, Sangha AK et al (2016) Protocols for molecular modeling with Rosetta3 and RosettaScripts. Biochemistry 55(34):4748–4763. https://doi.org/10.1021/acs.biochem.6b00444
27. Chien EY, Liu W, Zhao Q, Katritch V, Han GW, Hanson MA, Shi L, Newman AH et al (2010) Structure of the human dopamine D3 receptor in complex with a D2/D3 selective antagonist. Science 330(6007):1091–1095. https://doi.org/10.1126/science.1197410
28. Miller-Gallacher JL, Nehme R, Warne T, Edwards PC, Schertler GF, Leslie AG, Tate CG (2014) The 2.1 A resolution structure of cyanopindolol-bound beta1-adrenoceptor identifies an intramembrane Na+ ion that stabilises the ligand-free receptor. PLoS One 9(3):e92727. https://doi.org/10.1371/journal.pone.0092727
29. Cherezov V, Rosenbaum DM, Hanson MA, Rasmussen SG, Thian FS, Kobilka TS, Choi HJ, Kuhn P et al (2007) High-resolution crystal structure of an engineered human beta2-adrenergic G protein-coupled receptor. Science 318(5854):1258–1265. https://doi.org/10.1126/science.1150577
30. Wang C, Jiang Y, Ma J, Wu H, Wacker D, Katritch V, Han GW, Liu W et al (2013) Structural basis for molecular recognition at serotonin receptors. Science 340(6132):610–614. https://doi.org/10.1126/science.1232807
31. Wacker D, Wang C, Katritch V, Han GW, Huang XP, Vardy E, McCorvy JD, Jiang Y et al (2013) Structural features for functional selectivity at serotonin receptors. Science 340(6132):615–619. https://doi.org/10.1126/science.1232808
32. Kothiwale S, Mendenhall JL, Meiler J (2015) BCL::Conf: small molecule conformational sampling using a knowledge based rotamer library. J Cheminform 7:47. https://doi.org/10.1186/s13321-015-0095-1
33. Meiler J, Baker D (2006) ROSETTALIGAND: protein-small molecule docking with full side-chain flexibility. Proteins 65(3):538–548. https://doi.org/10.1002/prot.21086
34. Lemmon G, Meiler J (2012) Rosetta Ligand docking with flexible XML protocols. Methods Mol Biol 819:143–155. https://doi.org/10.1007/978-1-61779-465-0_10
35. Meador-Woodruff JH, Damask SP, Wang J, Haroutunian V, Davis KL Watson SJ (1996) Dopamine receptor mRNA expression in human striatum and neocortex. Neuropsychopharmacology 15:17–29
36. Pohjanoksa K, Jansson CC, Luomala K, Marjamaki A, Savola JM, Scheinin M (1997) Alpha2-adrenoceptor regulation of adenylyl cyclase in CHO cells: dependence on receptor density, receptor subtype and current activity of adenylyl cyclase. Eur J Pharmacol 335(1):53–63
37. Kukkonen JP, Renvaktar A, Shariatmadari R, Akerman KE (1998) Ligand- and subtype-selective coupling of human alpha-2 adrenoceptors to Ca++ elevation in Chinese hamster ovary cells. J Pharmacol Exp Ther 287(2):667–671
38. Schröder R, Schmidt J, Blättermann S, Peters L, Janssen N, Grundmann M, Seemann W, Kaufel D et al (2011) Applying label-free dynamic mass redistribution technology to frame signaling of G protein-coupled receptors noninvasively in living cells. Nat Protoc 6(11):1748–1760. https://doi.org/10.1038/nprot.2011.386
39. Atwood BK, Lopez J, Wager-Miller J, Mackie K, Straiker A (2011) Expression of G protein-coupled receptors and related proteins in HEK293, AtT20, BV2, and N18 cell lines as revealed by microarray analysis. BMC Genomics 12:14. https://doi.org/10.1186/1471-2164-12-14
40. Fraser CM, Arakawa S, McCombie WR, Venter JC (1989) Cloning, sequence analysis, and permanent expression of a human alpha 2-adrenergic receptor in Chinese hamster ovary cells. Evidence for independent pathways of receptor coupling to adenylate cyclase attenuation and activation. J Biol Chem 264(20):11754–11761

41. Jones SB, Halenda SP, Bylund DB (1991) Alpha 2-adrenergic receptor stimulation of phospholipase A2 and of adenylate cyclase in transfected Chinese hamster ovary cells is mediated by different mechanisms. Mol Pharmacol 39(2):239–245
42. Eason MG, Jacinto MT, Liggett SB (1994) Contribution of ligand structure to activation of alpha 2-adrenergic receptor subtype coupling to Gs. Mol Pharmacol 45(4):696–702
43. Eason MG, Kurose H, Holt BD, Raymond JR, Liggett SB (1992) Simultaneous coupling of alpha 2-adrenergic receptors to two G-proteins with opposing effects. Subtype-selective coupling of alpha 2C10, alpha 2C4, and alpha 2C2 adrenergic receptors to Gi and Gs. J Biol Chem 267(22):15795–11580
44. Eason MG, Liggett SB (1995) Identification of a Gs coupling domain in the amino terminus of the third intracellular loop of the alpha 2A-adrenergic receptor. Evidence for distinct structural determinants that confer Gs versus Gi coupling. J Biol Chem 270(42): 24753–24760
45. Leaver-Fay A, Tyka M, Lewis SM, Lange OF, Thompson J, Jacak R, Kaufman K, Renfrew PD et al (2011) ROSETTA3: an object-oriented software suite for the simulation and design of macromolecules. Methods Enzymol 487:545–574
46. Ring AM, Manglik A, Kruse AC, Enos MD, Weis WI, Garcia KC, Kobilka BK (2013) Adrenaline-activated structure of beta2-adrenoceptor stabilized by an engineered nanobody. Nature 502(7472):575–579. https://doi.org/10.1038/nature12572
47. Feng Z, Hou T, Li Y (2012) Selectivity and activation of dopamine D3R from molecular dynamics. J Mol Model 18(12):5051–5063. https://doi.org/10.1007/s00894-012-1509-x
48. Owesson-White CA, Roitman MF, Sombers LA, Belle AM, Keithley RB, Peele JL, Carelli RM, Wightman RM (2012) Sources contributing to the average extracellular concentration of dopamine in the nucleus accumbens. J Neurochem 121(2):252–262. https://doi.org/10.1111/j.1471-4159.2012.07677.x
49. Rice ME, Patel JC, Cragg SJ (2011) Dopamine release in the basal ganglia. Neuroscience 198:112–137. https://doi.org/10.1016/j.neuroscience.2011.08.066
50. Hersch SM, Ciliax BJ, Gutekunst CA, Rees HD, Heilman CJ, Yung KK, Bolam JP, Ince E et al (1995) Electron microscopic analysis of D1 and D2 dopamine receptor proteins in the dorsal striatum and their synaptic relationships with motor corticostriatal afferents. J Neurosci 15(7 Pt 2):5222–5237. https://doi.org/10.1016/b978-0-12-381270-4.00019-6
51. Yung KK, Bolam JP, Smith AD, Hersch SM, Ciliax BJ, Levey AI (1995) Immunocytochemical localization of D1 and D2 dopamine receptors in the basal ganglia of the rat: light and electron microscopy. Neuroscience 65(3):709–730
52. Goldman-Rakic PS, Lidow MS, Smiley JF, Williams MS (1992) The anatomy of dopamine in monkey and human prefrontal cortex. J Neural Transm Suppl 36:163–177
53. Castelli MP, Spiga S, Perra A, Madeddu C, Mulas G, Ennas MG, Gessa GL (2016) alpha2A adrenergic receptors highly expressed in mesoprefrontal dopamine neurons. Neuroscience 332:130–139. https://doi.org/10.1016/j.neuroscience.2016.06.037
54. Lee A, Wissekerke AE, Rosin DL, Lynch KR (1998) Localization of alpha2C-adrenergic receptor immunoreactivity in catecholaminergic neurons in the rat central nervous system. Neuroscience 84(4): 1085–1096
55. Brennan AR, Arnsten AF (2008) Neuronal mechanisms underlying attention deficit hyperactivity disorder: the influence of arousal on prefrontal cortical function. Ann N Y Acad Sci 1129:236–245. https://doi.org/10.1196/annals.1417.007
56. Herve D (2011) Identification of a specific assembly of the g protein golf as a critical and regulated module of dopamine and adenosine-activated cAMP pathways in the striatum. Front Neuroanat 5:48. https://doi.org/10.3389/fnana.2011.00048